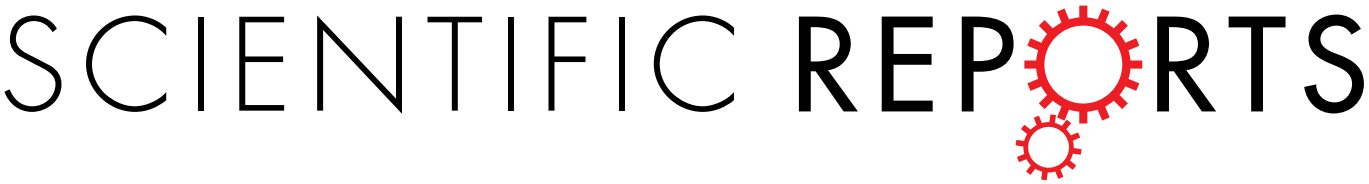

OPEN

Glass-on-Glass Fabrication of Bottle-Shaped Tunable Microlasers and their Applications

Received: 22 January 2016
Accepted: 11 April 2016
Published: 28 April 2016

Jonathan M. Ward[1], Yong Yang[1,2] & Síle Nic Chormaic[1]

We describe a novel method for making microbottle-shaped lasers by using a CO_2 laser to melt Er:Yb glass onto silica microcapillaries or fibres. This is realised by the fact that the two glasses have different melting points. The CO_2 laser power is controlled to flow the doped glass around the silica cylinder. In the case of a capillary, the resulting geometry is a hollow, microbottle-shaped resonator. This is a simple method for fabricating a number of glass whispering gallery mode (WGM) lasers with a wide range of sizes on a single, micron-scale structure. The Er:Yb doped glass outer layer is pumped at 980 nm via a tapered optical fibre and WGM lasing is recorded around 1535 nm. This structure facilitates a new way to thermo-optically tune the microlaser modes by passing gas through the capillary. The cooling effect of the gas flow shifts the WGMs towards shorter wavelengths and thermal tuning of the lasing modes over 70 GHz is achieved. Results are fitted using the theory of hot wire anemometry, allowing the flow rate to be calibrated with a flow sensitivity as high as 72 GHz/sccm. Strain tuning of the microlaser modes by up to 60 GHz is also demonstrated.

The fabrication of doped glass whispering gallery microlasers can be achieved in a limited number of ways. One method involves making a single cavity by drawing out a glass wire from a piece of doped glass and melting the tip of the wire to form a spherical resonator[1]. Alternatively, many spherical resonators can be made simultaneously by passing particles of doped glass through a furnace[2,3]. Both of these methods are tedious; in the first case, only one resonator can be made at a time. In the second case, individual spheres must be selected and glued to some other structure, e.g. the tip of a fibre, for ease of manipulation. Coating a tapered optical fibre tip with a layer of erbium doped phosphate glass and then melting the tip into a sphere has also been demonstrated to produce lasing microspheres[4,5]. For these methods, only a single resonator is selected and brought to an evanescent waveguide coupler for optical excitation. Individual doped glass WGM microlasers can also be made via femtosecond laser micromachining on a bulk sample of doped glass[6]. Simultaneous on-chip fabrication, by lithography and etching, of a large number of active glass resonators is possible by doping the chip before fabrication either with ion implantation[7] or by Solgel coating[8,9]. For passive devices, individual resonators - such as microspheres - can also be activated by coating using the Solgel process[10–12].The on-chip method is obviously more complicated and requires much more equipment than the simple heating methods, but it has the advantage that the coupling between the excitation waveguide and any cavity on the chip can be easily achieved by moving the chip relative to the waveguide.

Here, we present a simple heating method for fabricating a number of glass whispering gallery mode (WGM) lasers with a range of sizes on a single micron-scale structure that can be easily manipulated relative to the excitation waveguide and can, in principle, be packaged onto a millimetre scale chip. We experimentally demonstrate the coating of tapered optical fibres and microcapillaries with a layer of Er:Yb doped phosphate laser glass. This is achieved by the simple fact that the two glasses have very different melting temperatures, around 1500°C for silica and 500°C for the phosphate glass. The process is somewhat similar to the wetting method used for making polymer microresonators[13–16]. The Er:Yb doped glass outer layer is pumped at 980 nm and lasing is observed at 1535 nm. Microlasers with diameters ranging from 22 μm to 232 μm are made on the same structure.

A desired feature of any laser is the ability to tune the frequency of the laser output. Tuning a micron-scale whispering gallery resonator in a fashion that does not add to the footprint of the device or require complicated

[1]Light-Matter Interactions Unit, Okinawa Institute of Science and Technology Graduate University, Onna, Okinawa 904-0495, Japan. [2]National Engineering Laboratory for Fiber Optics Sensing Technology, Wuhan University of Technology, Wuhan, 430070, China. Correspondence and requests for materials should be addressed to J.M.W. (email: jonathan.ward@oist.jp)

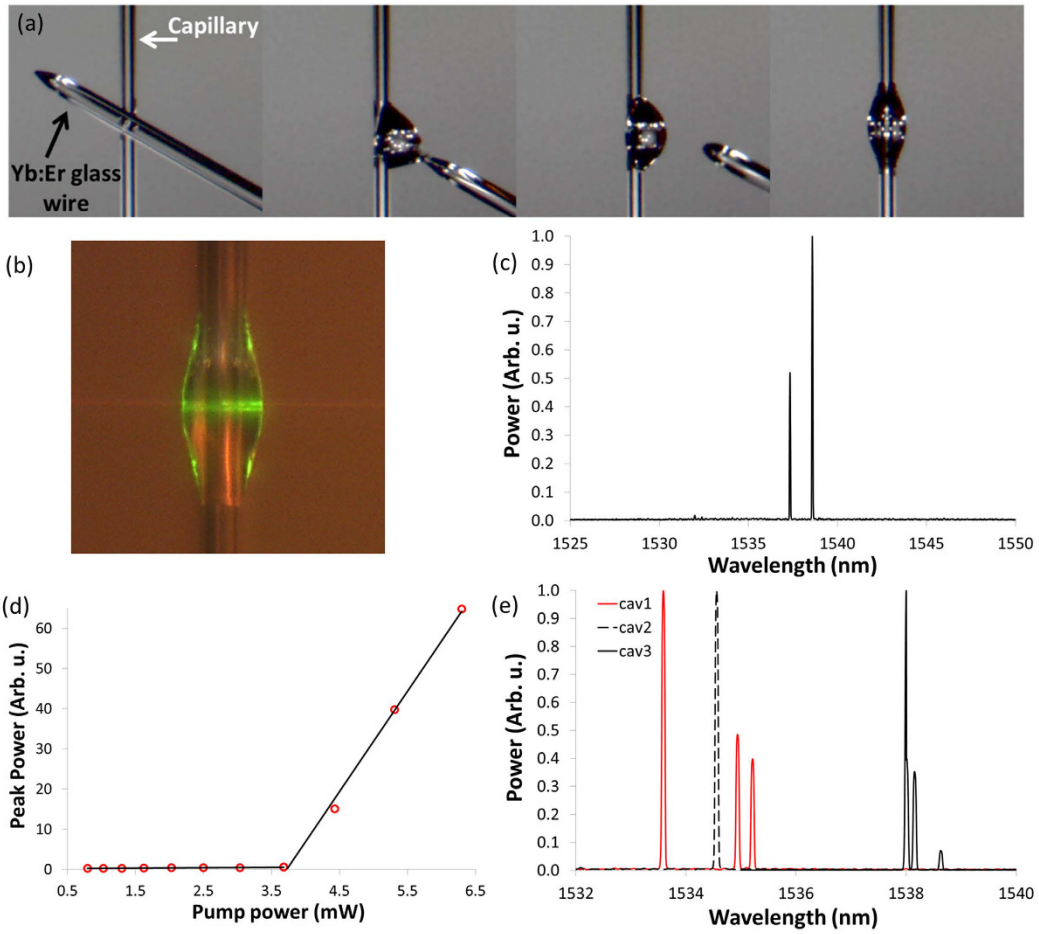

Figure 1. (**a**) Fabrication steps for making a doped glass microbottle laser on a silica wire, see supplementary file S1. The capillary diameter is 80 μm and the final diameter of the doped glass resonator is 170 μm. (**b**) Image of the resonator showing a WGM highlighted by green upconversion fluorescence. (**c**) Lasing spectrum from an Er:Yb doped bottle shaped resonator on a silica capillary. (**d**) Lasing threshold measurement. (**e**) Lasing spectra for three different microbottles on a single capillary with a diameter of 42 μm. The diameters of cav1, cav2 and cav3 are 120 μm, 170 μm and 155 μm, respectively.

fabrication is a nontrivial task. The main approaches so far include the use of external heaters[17,18], application of stress/strain via an external clamp[19–22], pressure tuning[23–27], electric field tuning[28], chemical etching[29,30], on-chip resistance heating[31,32], photorefractive tuning[33] and thermo-optic tuning[34–36]. Each of these methods has its own distinct advantages and disadvantages and the choice of method depends ultimately on the final application. We show that the microlasers fabricated using the glass-on-glass technique can be easily tuned over tens of GHz by one of two methods. The first method is unique to our devices and is applicable to the capillary structure; it relies on thermal tuning of the lasing mode by flowing gas through the cavity. From this method we demonstrate the idea of gas flow sensing using the concept of a "hot cavity" anemometer. Measurements and characterisation of the system as a gas flow sensor are presented. The second method relies on strain tuning and can be applied to both the tapered fibre and the capillary lasers.

Methods

The method of microlaser fabrication can be applied to an optical fibre or capillary and is the same in both cases. First, we tapered a microcapillary with an outer diameter (OD) of 350 μm and an inner diameter (ID) of 250 μm, using a CO_2 laser, to a uniform waist with an OD of ~80 μm. Next, a glass wire was drawn from a bulk piece of Er:Yb doped phosphate glass[37]. The diameter of the doped glass wire was typically a few tens of microns. This glass wire was then placed on top of, and in contact with, the microcapillary and the CO_2 laser beams were applied again. The CO_2 laser power was increased until the doped glass flowed onto the capillary, as shown in Fig. 1(a). At this point, the doped glass wire was removed and the CO_2 laser power was controlled to allow the remaining doped glass to flow around the capillary. When the doped glass completely covered the capillary the CO_2 laser was turned off. The resulting geometry was a hollow, microbottle-shaped resonator. The diameter of the doped glass bottle was 170 μm and the thickness of the doped glass at the equator was 40 μm. This thick layer means that any optical mode in the bottle cannot interact with the silica or any material inside the capillary.

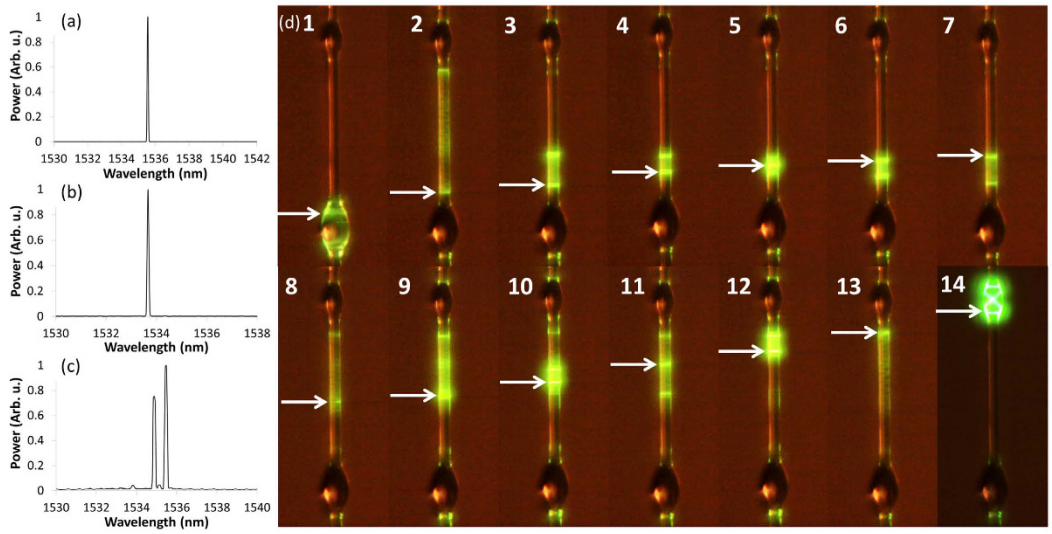

Figure 2. (**a–c**) Lasing spectra from three of five resonators made on the same 20 μm fibre. The spectra correspond to bottle resonators with diameters of 42 μm (top), 60 μm (middle) and 160 μm (bottom). (**d**) The excitation of a continuous series of microresonators from thickness variations in a thin coating. Each panel (1–14) is an image of a 20 μm fibre supporting two microbottles, one at the top and one at the bottom of the image. In between these two resonators is a region with a thin coating of doped glass and the tapered fibre (white arrow) is moved along this region, see supplementary file S2. The lasing spectra in (**a**,**b**) correspond to the taper positions indicated in panel 1 and 14, respectively.

The capillary was glued onto a U-shaped holder and brought into contact with a tapered optical fibre for optical pumping. The tapered fibre had a diameter of ~1 μm and was connected to a 980 nm diode laser. Whispering gallery modes were visible due to green upconversion fluorescence from the erbium ions, see Fig. 1(b). The output end of the tapered fibre was connected to an optical spectrum analyser (OSA). A typical lasing spectrum is shown in Fig. 1(c), with lasing peaks appearing between 1532 nm and 1540 nm. For a given microbottle, the spectrum can be single mode or multimode depending on the pump power and the coupling condition[10,12,33], i.e. the thickness of the tapered fibre or the position of the taper relative to the bottle's equator. To verify the lasing behaviour, a threshold measurement was taken, see Fig. 1(d). For this measurement the pump laser was not tuned to any particular WGM. The 980 nm pump laser used had a rated linewidth of 2 nm so it was assumed that a number of WGMs were simultaneously excited with no control over the coupling efficiency. As such, the pump power labled in Fig. 1(d) represents the pump power launched into the tapered fibre and does not represent the true pump power lasing threshold. Figure 1(d) does, however, show a clear threshold for the peak output power.

By repeating the fabrication process at different points along a capillary it is possible to make a string of resonators in a row. As a demonstration, three resonators with diameters of 120 μm, 170 μm and 155 μm were made on the same capillary, which had an OD of 42 μm. Lasing was excited in each resonator in turn by simply moving the tapered fibre along the capillary to the next resonator. Lasing was collected from each resonator for the same tapered fibre diameter and for the same pump power, see Fig. 1(e).

The same fabrication steps were repeated for an optical fibre. In this case, a standard single mode optical fibre was tapered using a CO_2 laser to a diameter of 20 μm. The same erbium-doped glass was melted on the tapered fibre at five different points creating five separate cavities with diameters ranging from 42 μm to 232 μm. Figure 2(a–c) shows the WGM lasing spectra taken for three of these resonators collected using the same pump power and position on the tapered fibre; note that the remaining two cavities only showed fluorescence under these conditions.

Apart from making a bottle-shaped or spherical resonator, it was also possible to apply a thin coating of the doped glass. This was achieved by heating the sphere of doped glass after it had been transferred to the fibre (or capillary). This additional heating caused the sphere to move along the fibre leaving behind a thin layer surrounding the 20 μm fibre. The thickness of this layer is not constant so microcavities are formed by the small variations in the diameter, similar to SNAP structures[38]. Figure 2(d) shows such a thin layer spread out between two microlasers. The position of the excitation tapered fibre, represented by the white white arrow, was moved along this thinly-coated region. The thickness of the doped layer was measured using an optical microscope and was determined to be around 1–2 μm. At each position a WGM spectrum was observed and, at some positions, lasing was achieved. In the future, it may be desirable to make a more accurate measurement of the diameter from the variations in the WGM spectra at each position.

Results

Thermo-optical tuning and gas flow sensing. Hollow whispering gallery resonators, such as microcapillaries[39] and microbubbles[40–42], have the unique feature that a material can fill or flow through their inner volume as already demonstrated for dye-filled microbubble lasers[43], capillaries[44] and on-chip microfluidic channels[45].

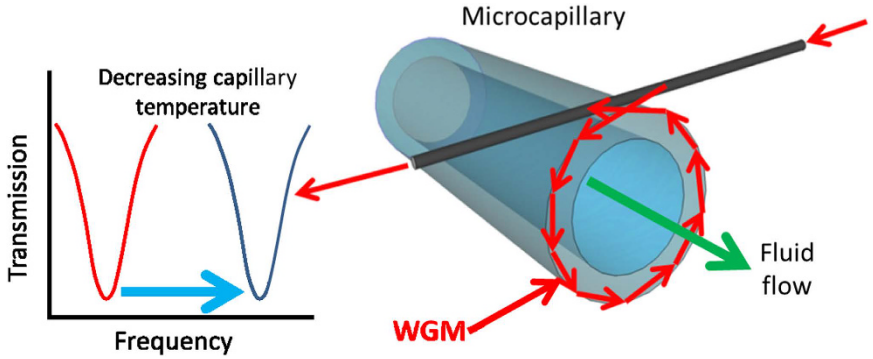

Figure 3. Schematic of a WGM "hot cavity" anemometer. The excitation of the WGM is represented by the red arrows in the capillary wall. With sufficient absorption, the light in the WGM can locally heat the capillary. Fluid flowing through the capillary is represented by the green arrow. The flowing fluid removes the heat and shifts the WGMs to higher frequencies, represented by the movement of the transmission dip on the left of the figure.

The light travelling in the WGM is partially absorbed by the glass and locally increases the temperature of the resonator's wall. When fluid flows through the resonator it removes some of the heat and reduces the temperature. This causes a blue shift in the frequency of the WGM. In this way the WGMs can be tuned and the shift can be calibrated to represent the flow rate of the fluid, with larger flow rates giving larger blue shifts, see Fig. 3.

This is similar to the concept of all-optical, hot wire anemometry, a method which has been in use for some time. Most of the reported devices are based on a SiO_2 optical waveguide, which is treated as a wire that absorbs light thereby creating heat[46–50]. The wire is placed into, or in contact with, a fluid flow channel. The flow of the fluid cools the wire and this changes the refractive index or the length of the wire. Such changes can be read out optically using a fibre Bragg grating (FBG), for example[46–50]. Because SiO_2 is generally not a strong absorber, a significant amount of optical power is required to generate heat. The process can be aided by the addition of a metal[46–50]. Most of the systems discussed above are not capable of measuring flow in arbitrarily small channels such as one would find in microfluidic systems, though recently a FBG hot wire anemometer was used to measure flow in such a system[50]. Although the sensor showed good sensitivity in the low flow rate regime, the device required hundreds of mW of pump power, the resolution was low, and good thermal contact had to be maintained between the optical absorber and the flow channel. A hot cavity anemometer that can be incorporated onto a microcapillary automatically provides good thermal overlap between the sensor and the flow channel. For an Er:Yb doped resonator, significant heat is generated by pump absorption at 980 nm and a narrow linewidth lasing mode at 1535 nm is used to measure the thermo-optical shift of the cavity modes induced by the flow of fluid through the capillary. This device offers high resolution (by using the lasing modes) and high sensitivity (due to the high temperatures) with low pump powers.

It is well-known that there are a number of large non-radiative energy transitions in erbium-doped glass which can be accessed by pumping at 980 nm[51–53]. These phonon transitions generate a significant amount of heat in the glass even for low pump powers; in fact up to 40% of the optical pump power can be converted to heat. By flowing a gas/fluid through the capillary this heat is partially removed and the WGMs shift at a rate determined by the thermo-optical behaviour ($\beta = dn/dT = -21 \times 10^{-7}\,K^{-1}$) and the thermal contraction ($\alpha = dr/dT = 114 \times 10^{-7}\,K^{-1}$) of the glass. Based on the coefficients given by the manufacturer[37] the thermal shift rate of the WGMs should be around 0.0145 nm/K (or 1.9 GHz/K) at 1535 nm, where the shift is defined as[51,54]

$$\Delta\lambda = (\alpha + \beta)\Delta T, \tag{1}$$

and ΔT is the change in cavity temperature. The capillary with the microlaser shown in Fig. 1(a,b) was connected to a source of pressurised air via a pressure regulator. The output of the capillary was connected to a mass flow meter. The shift of the lasing peaks was recorded on the OSA as the pump power was increased. This was done with no air flowing through the capillary and for increasing flow rates, with the results plotted in Fig. 4(a). For this particular cavity, the shift rate of the WGMs goes from −16.2 GHz/mW to −4.1 GHz/mW for zero flow and 15 sccm, respectively. Using Eq. 1 the change in temperature of the cavity for the maximum shift in each case can be estimated and is plotted in Fig. 4(b). With no gas flow the temperature increases by 66°C, whereas with a maximum flow rate of 15 sccm the maximum temperature increase was reduced to 13°C. Next, the input pump power was fixed and the input pressure to the capillary was increased while the positions of the WGMs in the transmitted signal were recorded using the OSA. As the flow rate increased the WGMs were observed to shift towards shorter wavelengths due to the cooling effect of the air flow through the capillary, as discussed above. This procedure was repeated for increasing pump powers and the results are plotted in Fig. 4(c).

From the theory of optical hot wire anemometry[46,50], the heat lost, H, from a hot wire is related to the flow rate, f, by

$$H = (A + Bf^n)\Delta T_a \tag{2}$$

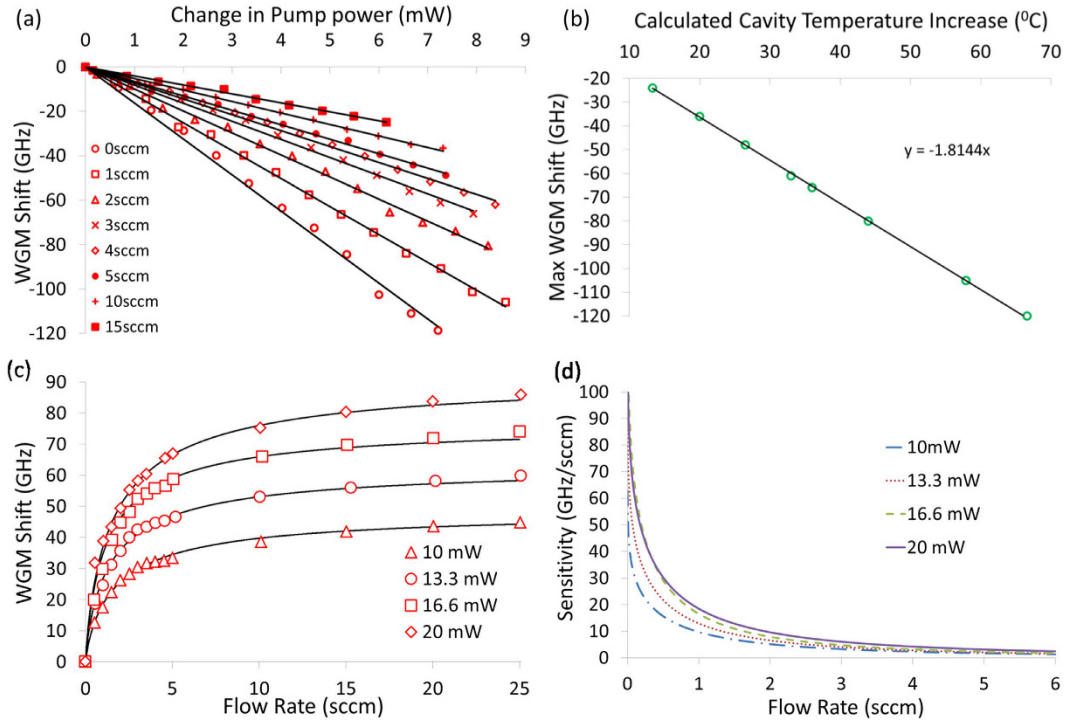

Figure 4. (**a**) The shift rate of the 1535 nm lasing WGM as function of input pump power for different gas flow rates. (**b**) The calculated increase in cavity temperature and corresponding WGM shifts. (**c**) The shift of the 1535 nm lasing WGM as function of the measured flow rate for different pump powers, solid lines are fits. (**d**) The sensitivity of the WGM shift rate as function of measured flow rate, calculated from the derivative of the, solid lines are fits in (**c**).

where A and B are empirical constants and n is a fitting parameter (usually 0.5 for a simple hot wire). A certain amount of pump power is used to generate the lasing signal so the cavity is already heated, thus the initial temperature of the cavity is not known. Even for modest pumping the initial cavity temperature can be easily greater than 100°C[55]. Therefore, we define $\Delta T_a = [T_a(f) - T_a(f=0)]$, i.e. the difference between the cavity temperature at zero flow and the cavity temperature at some flow rate, f. Based on the law of energy conservation the heat lost must equal the heat acquired. Therefore, in the case of the WGM resonator

$$H = I\eta(Q/Q_{abs}), \tag{3}$$

where I is the input power, η is the coupling efficiency, Q is the quality factor of the cavity and Q_{abs} is the absorption-limited cavity quality factor given by

$$Q_{abs} = \frac{2\pi n_{eff}}{\sigma\lambda}, \tag{4}$$

where σ is the absorption loss of the material, λ is the wavelength and n_{eff} is the effective refractive index. σ was estimated from the glass material properties provided by the manufacturer[37] using an absorbing ion concentration of 3×10^{21} ions/cm^3 and an absorption cross-section of 1.7×10^{20}/cm^2. The calculated $Q_{abs} = 1.2 \times 10^6$ and the loaded cavity Q was assumed to be 100 times less than this. To determine ΔT_a, the change in temperature for each pump power was determined from the maximum shift and Eq. 1. The WGM shift in terms of the gas flow rate can then be written as[46,50]

$$\delta\lambda = \lambda(\alpha + \beta)[H/(A + Bf^n) - \Delta T_a]. \tag{5}$$

The recorded WGM shifts were fitted using Eq. 5, see solid lines in Fig. 4(c). The 980 nm pump laser used in the experiment had a rated linewidth of 2 nm, therefore the coupling efficiency of the pump to a specific WGM was impossible to quantify. For fitting we assumed a coupling efficiency of 20%. This value is justified by the fact that we observe about a 20–30% dip in transmitted power when the taper and microbottle make contact. The fitting parameter n was set to 0.84. Using these parameters the corresponding fits agree with the observed shift. The sensitivities of the WGM shift rates are determined by differentiating the fits in Fig. 4(c) and are plotted in Fig. 4(d). As can be seen from Fig. 4(d), the sensitivity to changes in flow is highest for flow rates below 2 sccm. The smallest flow rate measurable with the mass flow meter is 0.5 sccm and this produced a 30 GHz shift of the WGMs, see Fig. 4(c). At a flow rate of 0.01 sccm (10 μL/min) the sensitivity is 72 GHz/sccm (Fig. 4(d)). At this

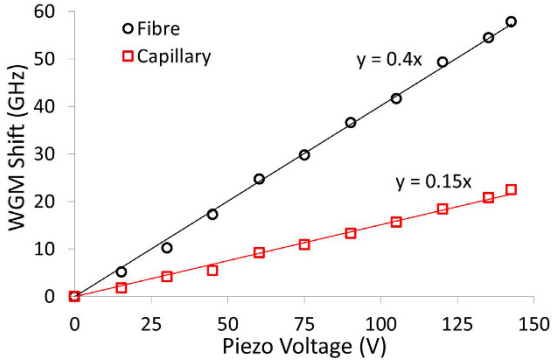

Figure 5. Strain tuning of a 42 μm diameter microlaser on an optical fibre (empty black circles) with a diameter of 20 μm and strain tuning of a 120 μm diameter microlaser on a capillary (empty red squares) with a diameter of 42 μm. Solid lines are linear fits.

sensitivity a change of 0.01 sccm should produce a shift of around 1.5 GHz, which is just about readable using the peak tracking function on the OSA.

Strain tuning. Strain tuning of microresonators is an effective, fast and stable tuning method and has been reported previously for passive glass microcavities[19,20,22,24,25], as well as for passive and doped polymer cavities[21,56,57]. Its use for tuning doped glass resonators has been limited[26,58]. Strain tuning of an erbium-doped microbottle laser was reported by Pöllinger *et al.*[58]. However, etching using hydrofluoric acid was needed to access the core of an erbium-doped fibre which was subsequently melted by a CO_2 laser to form the bottle shape. In our work, no etching is required and a large number of microlasers with a wide range of sizes can be made quickly and easily. The 20 μm diameter fibre with the five microlasers, as described earlier, was held on a stage that allowed the U-shaped mount holding the fibre to be extended, thereby putting strain on the fibre. The extension was achieved using a piezo stack that provided 17 μm displacement. The 42 μm diameter microlaser was selected and coupled to the tapered optical fibre and its lasing output was monitored while a voltage was applied to the piezo stack. The same procedure was applied to the 42 μm capillary supporting the three microlasers; in this case the 120 μm diameter microlaser was selected for tuning. The tuning curves for both microlasers are shown in Fig. 5.

The 42 μm diameter microlaser on the tapered fibre showed a larger tuning of around 60 GHz, most likely due to its smaller diameter of the fibre. However, a number of factors could influence the final tuning range, e.g. the diameter of the taper and the initial tension on the taper. For the capillary, the diameter and the wall thickness may also play a role. The silica fibre/capillary and the doped glass microbottles are not a single structure so this may act to further reduce the final tuning range. Nevertheless, a significantly usable tuning range was achieved. The change in the size of the resonator can be estimated from the expression[22]

$$\Delta\nu = \frac{\Delta d}{d}\nu, \tag{6}$$

where $\Delta\nu$ is the frequency shift, Δd is the change in diameter, d is the diameter and ν is the frequency. The 60 GHz shift for the 42 μm diamater bottle on the 20 μm tapered fibre equates to a diameter change of 13 pm and an effective Poisson ratio, $\Delta d/\Delta z = 7.6 \times 10^{-7}$, where Δz is the 17 μm displacement of the piezo actuator. The Poisson ratio of the phosphate glass is 0.24[37] and silica is 0.17. The shift rate of the modes is estimated as 3.5 GHz/μm (at 1535 nm) and this can be compared to the strain-induced shift rate of 6 GHz/μm (at 637 nm)[22] for a thin-stemmed, silica sphere and a 100 GHz/μm (at 800 nm)[19] for a thick-stemmed, silica sphere.

Discussion

We have presented a method for creating glass-on-glass structures, such as bottle resonators or thin coatings, where one glass is melted and allowed to flow onto another tightly curved glass structure. This is achieved by the fact that the two glass have significantly different melting points; therefore, this method should also be applicable to other soft glasses. For example, high index glasses such as lead silicate or tellurite could be formed into small cavities on a tapered fibre with diameters around 20 μm. The number of resonators on a single fibre depends on the size of the resonator and length of the fibre. So far, we can place each cavity approximately 100 μm apart. One could envision fibres, each with a number of microlasers, mounted on a chip consisting of waveguides for addressing each resonator.

The ability to make hollow, microbottle-shaped, doped glass microlasers allows us to investigate a new method of thermo-optical tuning where the lasing modes can be tuned by simply flowing air through the cavity. The thickness of the capillary wall and a thick, doped glass layer negates any red shift of the optical mode induced by increases in internal pressure. We demonstrated that the mode shifts can be calibrated to represent the gas flow rate, thus creating an integrated, all-optical, flow sensor with low power and high resolution. The measurement of liquid flow is also possible with this setup and we have seen a water flow rate sensitivity of 1 GHz/(nL/sec) in a capillary with an ID of 100 μm. Early tests of strain tuning also show promising results and further studies should reveal the dependence of the tuning range on the fibre diameter, size of the resonator and wall thickness of the

microcapillary. In future work we plan to explore this method further using various soft glasses and structures to study the possibility of creating new and interesting glass-on-glass devices. For example, it may be possible to flow melted glass into channels which have been pre-etched in silica glass.

References

1. Chen, S., Sun, T., Grattan, K., Annapurna, K. & Sen, R. Characteristics of Er and Er–Yb–Cr doped phosphate microsphere fibre lasers. *Optics Communications* **282,** 3765–3769 (2009).
2. Lissillour, F. *et al.* Whispering-gallery mode Nd-ZBLAN microlasers at 1.05 μm. *Proceedings of SPIE Conference on Infrared Glass Optical Fibers and Their Applications, Québec, Canada, SPIE* **3416,** 150–156 (September, 28, 1998).
3. Ward, J. M., Wu, Y., Khalfi, K. & Nic Chormaic, S. Short vertical tube furnace for the fabrication of doped glass microsphere lasers. *The Review of Scientific Instruments* **81,** 073106, doi: 10.1063/1.3455198 (2010).
4. Dong, C.-H. *et al.* Low-Threshold Microlaser in Er : Yb Phosphate. *IEEE Photonics Technology Letters* **20,** 342–344 (2008).
5. Dong, C. *et al.* Observation of microlaser with Er-doped phosphate glass coated microsphere pumped by 780 nm. *Optics Communications* **283,** 5117–5120 (2010).
6. Lin, J. *et al.* Low-threshold whispering-gallery-mode microlasers fabricated in a Nd:glass substrate by three-dimensional femtosecond laser micromachining. *Optics Letters* **38,** 1458–60 (2013).
7. Min, B. *et al.* Erbium-implanted high-Q silica toroidal microcavity laser on a silicon chip. *Physical Review A* **70,** 1–12 (2004).
8. Yang, L., Carmon, T., Min, B., Spillane, S. M. & Vahala, K. J. Erbium-doped and Raman microlasers on a silicon chip fabricated by the sol-gel process. *Applied Physics Letters* **86,** 091114, doi: 10.1063/1.1873043 (2005).
9. Zheng, B. *et al.* A chip-based microcavity derived from multi-component tellurite glass. *Journal of Materials Chemistry C* **3,** 5141–5144 (2015).
10. Yang, L. & Vahala, K. J. Gain functionalization of silica microresonators. *Optics Letters* **28,** 592–4 (2003).
11. Fan, H., Hua, S., Jiang, X. & Xiao, M. Demonstration of an erbium-doped microsphere laser on a silicon chip. *Laser Physics Letters* **10,** 105809, doi: 10.1088/1612-2011/10/10/105809 (2013).
12. Nunzi Conti, G. *et al.* Spectroscopic and lasing properties of Er3+-doped glass microspheres. *Journal of Non-Crystalline Solids* **352,** 2360–2363 (2006).
13. Gu, G. *et al.* Fabrication of ultraviolet-curable adhesive bottle-like microresonators by wetting and photocuring. *Applied Optics* **53,** 7819–7824 (2014).
14. Lu, Q., Wu, X., Liu, L. & Xu, L. Mode-selective lasing in high-Q polymer micro bottle resonators. *Optics Express* **23,** 22740 (2015).
15. Grimaldi, I. A. *et al.* Polymer based planar coupling of self-assembled bottle microresonators. *Applied Physics Letters* **105,** 2012–2016 (2014).
16. Frenkel, M., Avellan, M. & Guo, Z. Whispering-gallery mode composite sensors for on-chip dynamic temperature monitoring. *Measurement Science & Technology* **24,** 075103, doi: 10.1088/0957-0233/24/7/075103 (2013).
17. Chiba, A., Fujiwara, H., Hotta, J.-i., Takeuchi, S. & Sasaki, K. Resonant Frequency Control of a Microspherical Cavity by Temperature Adjustment. *Japanese Journal of Applied Physics* **43,** 6138–6141 (2004).
18. Suter, J. D., White, I. M., Zhu, H. & Fan, X. Thermal characterization of liquid core optical ring resonator sensors. *Applied Optics* **46,** 389–96 (2007).
19. von Klitzing, W., Long, R., Ilchenko, V. S., Hare, J. & Lefèvre-Seguin, V. Frequency tuning of the whispering-gallery modes of silica microspheres for cavity quantum electrodynamics and spectroscopy. *Optics Letters* **26,** 166–168 (2001).
20. Sumetsky, M., Dulashko, Y. & Windeler, R. S. Super free spectral range tunable optical microbubble resonator. *Optics Letters* **35,** 1866–8 (2010).
21. Madugani, R. *et al.* Terahertz tuning of whispering gallery modes in a PDMS stand-alone, stretchable microsphere. *Optics Letters* **37,** 4762–4764 (2012).
22. Dinyari, K. N., Barbour, R. J., Golter, D. A. & Wang, H. Mechanical tuning of whispering gallery modes over a 0.5 THz tuning range with MHz resolution in a silica microsphere at cryogenic temperatures. *Optics Express* **19,** 17966–72 (2011).
23. Ioppolo, T. & Ötügen, M. V. Pressure tuning of whispering gallery mode resonators. *Journal of the Optical Society of America B* **24,** 2721–2726 (2007).
24. Henze, R., Seifert, T., Ward, J. & Benson, O. Tuning whispering gallery modes using internal aerostatic pressure. *Optics Letters* **36,** 4536–8 (2011).
25. Weigel, T., Esen, C., Schweiger, G. & Ostendorf, A. Whispering gallery mode pressure sensing. *Proceedings of SPIE - The International Society for Optical Engineering* **8439,** 1–6 (2012).
26. Martin, L. L. *et al.* High pressure tuning of whispering gallery mode resonances in a neodymium-doped glass microsphere. *Journal of the Optical Society of America B* **30,** 3254–3259 (2013).
27. Henze, R., Ward, J. M. & Benson, O. Temperature independent tuning of whispering gallery modes in a cryogenic environment. *Optics Express* **21,** 675–80 (2013).
28. Ioppolo, T., Ayaz, U. & Otügen, M. V. Tuning of whispering gallery modes of spherical resonators using an external electric field. *Optics Express* **17,** 16465–79 (2009).
29. White, I. M., Hanumegowda, N. M., Oveys, H. & Fan, X. Tuning whispering gallery modes in optical microspheres with chemical etching. *Optics Express* **13,** 10754–9 (2005).
30. Henze, R. *et al.* Fine-tuning of whispering gallery modes in on-chip silica microdisk resonators within a full spectral range. *Applied Physics Letters* **102,** 041104, doi: 10.1063/1.4789755 (2013).
31. Armani, D., Min, B., Martin, A. & Vahala, K. J. Electrical thermo-optic tuning of ultrahigh-Q microtoroid resonators. *Applied Physics Letters* **85,** 5439–5441 (2004).
32. Shainline, J. M., Fernandes, G., Liu, Z. & Xu, J. Broad tuning of whispering-gallery modes in silicon microdisks. *Optics Express* **18,** 14345–52 (2010).
33. Ristić, D. *et al.* Photoluminescence and lasing in whispering gallery mode glass microspherical resonators. *Journal of Luminescence* **170,** 755–760 (2015).
34. Dong, C.-H. *et al.* Fabrication of high-Q polydimethylsiloxane optical microspheres for thermal sensing. *Applied Physics Letters* **94,** 231119, doi: 10.1063/1.3152791 (2009).
35. Li, B. B. *et al.* On chip, high-sensitivity thermal sensor based on high- Q polydimethylsiloxane-coated microresonator. *Applied Physics Letters* **96,** 251109, doi: 10.1063/1.3457444 (2010).
36. Watkins, A., Ward, J. & Nic Chormaic, S. Thermo-Optical Tuning of Whispering Gallery Modes in Erbium:Ytterbium Doped Glass Microspheres to Arbitrary Probe Wavelengths. *Japanese Journal of Applied Physics* **51,** 052501, doi: 10.1143/JJAP.51.052501 (2012).
37. Kigre Inc., kigre laser glass data sheet, http://www.kigre.com/products/laser_glass.pdf, date of access: 25/03/2016.
38. Sumetsky, M. & Fini, J. M. Surface nanoscale axial photonics. *Optics Express* **19,** 3–14 (2011).
39. Fan, X., White, I. M., Zhu, H., Suter, J. D. & Oveys, H. Overview of novel integrated optical ring resonator bio/chemical sensors. *Proceedings of SPIE - Laser Resonators and Beam Control IX* **6452,** 64520M1–20 (2007).
40. Sumetsky, M., Dulashko, Y. & Windeler, R. S. Optical microbubble resonator. *Optics letters* **35,** 898–900 (2010).
41. Yang, Y., Ward, J. & Nic Chormaic, S. Quasi-droplet microbubbles for high resolution sensing applications. *Optics Express* **22,** 6881–98 (2014).

42. Ward, J. M., Dhasmana, N. & Nic Chormaic, S. Hollow Core, Whispering Gallery Resonator *Sensors* **1935,** 14–16 (2014).
43. Lee, W. *et al.* A quasi-droplet optofluidic ring resonator laser using a micro-bubble. *Applied Physics Letters* **99,** 091102, doi: 10.1063/1.3629814 (2011).
44. Wu, X., Sun, Y., Suter, J. D. & Fan, X. Single mode coupled optofluidic ring resonator dye lasers. *Applied Physics Letters* **94,** 241109, doi: 10.1063/1.3156861 (2009).
45. Lee, W. *et al.* Tunable single mode lasing from an on-chip optofluidic ring resonator laser. *Applied Physics Letters* **98,** 061103, doi: 10.1063/1.3554362 (2011).
46. Gao, S., Zhang, A. P., Tam, H.-Y., Cho, L. H. & Lu, C. All-optical fiber anemometer based on laser heated fiber Bragg gratings. *Optics Express* **19,** 10124–10130 (2011).
47. Cheng, J., Zhu, W., Huang, Z. & Hu, P. Experimental and simulation study on thermal gas flowmeter based on fiber Bragg grating coated with silver film. *Sensors and Actuators A: Physical* **228,** 23–27 (2015).
48. Cashdollar, L. J. & Chen, K. P. Fiber Bragg grating flow sensors powered by in-fiber light. *IEEE Sensors Journal* **5,** 1327–1331 (2005).
49. Wang, X. *et al.* Hot-Wire Anemometer Based on Silver-Coated Fiber Bragg Grating Assisted by No-Core Fiber. *IEEE Photonics Technology Letters* **25,** 2458–2461 (2013).
50. Li, Y., Yan, G., Zhang, L. & He, S. Microfluidic flowmeter based on micro "hot-wire" sandwiched Fabry-Perot interferometer. *Optics Express* **23,** 9483–9493 (2015).
51. Cai, Z., Chardon, A., Xu, H., Patrice, F. & St, G. M. Laser characteristics at 1535 nm and thermal effects of an Er : Yb phosphate glass microchip pumped by Ti: sapphire laser. *Optics Communications* **203,** 301–313 (2002).
52. O'Shea, D. G. *et al.* Upconversion channels in Er3+:ZBLALiP fluoride glass microspheres. *The European Physical Journal Applied Physics* **40,** 181–188 (2007).
53. Ward, J. M., Wu, Y. & Nic Chormaic, S. Thermo-optical tuning of whispering gallery modes in erbium doped microspheres. *Applied Physics B: Lasers and Optics* **100,** 847–850 (2010).
54. Brenci, M. *et al.* Microspherical resonators for biophotonic sensors. *Proc. of SPIE* **6158,** 61580S, doi: 10.1117/12.675800 (2006).
55. Ward, J. M., Féron, P. & Nic Chormaic, S. A taper-fused microspherical laser source. *IEEE Photonics Technology Letters* **20,** 392–394 (2008).
56. Linslal, C. L. *et al.* Tuning whispering gallery lasing modes from polymer fibers under tensile strain. *Optics Letters* **41,** 551–554 (2016).
57. Zhou, Z. H., Shu, F. J., Shen, Z., Dong, C. H. & Guo, G. C. High-Q whispering gallery modes in a polymer microresonator with broad strain tuning. *Science China: Physics, Mechanics and Astronomy* **58,** 114208, doi: 10.1007/s11433-015-5725-0 (2015).
58. Pöllinger, M., O'Shea, D., Warken, F. & Rauschenbeutel, A. Ultrahigh-Q Tunable Whispering-Gallery-Mode Microresonator. *Physical Review Letters* **103,** 1–4 (2009).

Acknowledgements

This work was funded by the Okinawa Institute of Science and Technology Graduate University.

Author Contributions

J.M.W. conceived the experiment and did the data analysis; J.M.W. and Y.Y. conducted the measurements; S.N.C. supervised the project; all authors contributed to discussions on the project and manuscript preparation. All authors reviewed the manuscript.

Additional Information

Supplementary information accompanies this paper at http://www.nature.com/srep

Competing financial interests: The authors declare no competing financial interests.

How to cite this article: Ward, J. M. *et al.* Glass-on-Glass Fabrication of Bottle-Shaped Tunable Microlasers and their Applications. *Sci. Rep.* **6**, 25152; doi: 10.1038/srep25152 (2016).

SCIENTIFIC REPORTS

OPEN

Corrigendum: Glass-on-Glass Fabrication of Bottle-Shaped Tunable Microlasers and their Applications

Jonathan M. Ward, Yong Yang & Síle Nic Chormaic

Scientific Reports **6**:25152; doi: 10.1038/srep25152; published online 28 April 2016; updated on 23 January 2017

This Article contains an error in Figure 4b, which uses an inaccurate value for the glass thermo-optic coefficient.

The thermo-optic coefficient stated in the Article is $dn/dT = -21*10^{-7}K^{-1}$, however the value stated by the manufacturer is $dn/dT = -63*10^{-7}K^{-1}$ (for 20–40 °C). The calculated temperature of the resonator for a thermo-optic coefficient of $-63*10^{-7}K^{-1}$ (20–40 °C) changes the calculated mode shift rate from ~1.9 GHz/K to ~1 GHz/K, implying the cavity temperature is almost doubled.

The data points in Figure 4c are not affected, however the fitting curves are. These can be readjusted by modifying the fitting parameters to take into account the increased temperature. This can be done by altering the thermal expansion co-efficient from $114*10^{-7}K^{-1}$ (20–40 °C) to $119*10^{-7}K^{-1}$. The fitting parameter, n, remains as 0.84 by slightly decreasing the empirical calibration constants (A and B). The resulting change to the fitting curves is negligible.

The thermo-optic coefficient and the thermal expansion coefficient quoted by the manufacturer are given for a specific temperature range only (for 20–40 °C) and are known to vary outside this range. The authors' glass resonator is operating well outside this temperature range and so it is reasonable to adjust these coefficients for the purpose of fitting.

The correct Figure 4b appears below as Figure 1.

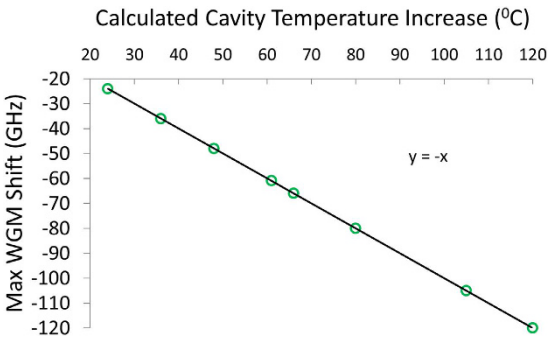

Figure 1.